

# Geostatistical lithofacies modeling of the upper sandstone member/Zubair formation in south Rumaila oil field, Iraq

Watheq J. Al-Mudhafar<sup>1,2</sup>

Received: 14 December 2016 / Accepted: 8 March 2017 / Published online: 21 March 2017  
© Saudi Society for Geosciences 2017

**Abstract** Geological facies modeling is a crucial problem for reservoir characterization as it affects the reservoir heterogeneities and fluid flow performance prediction. The main purpose of this research is to adopt a stochastic simulation to construct 3D lithofacies models of the tidal/estuarine depositional environment of the upper sandstone member in south Rumaila oil field, located in Iraq. Based on core measurements, the upper sandstone member has three main lithofacies: sand, shaly sand, and shale. Literature review indicates that the formation is encompassed of mainly sandstone with some inter-bedded shale zones. To reconstruct the 3D lithofacies model, the sequential indicator simulation (SISIM) was adopted to build the categorical image, pixel by pixel, considering the nonparametric condition distribution. Specifically, SISIM depends on the variogram to address and model the variation between any two spatial points from the available data. Therefore, 12 different variograms were constructed given the three lithofacies in four different azimuth directions: 0°, 45°, 90°, and 135°. The resulting lithofacies models in the four selected azimuth directions have shown frequent tidal lithofacies channeling and indicate an approximate matching with the original description of the formation depositional environment of the tidal-dominated and sand-rich environment. The generated lithofacies model in 135° direction has sand channels prevailing towards the south-east shoreline of the reservoir. The created lithofacies model also preserves the reservoir complexity and heterogeneity because it was created using a high-resolution gridding system

with approximately two million grids. Additionally, the resulting tidal lithofacies model ensures reservoir heterogeneity as the petrophysical properties are then distributed given each lithofacies with distinct indicator variograms.

**Keywords** Geostatistical lithofacies modeling · Sequential indicator simulation · Tidal depositional environment · Sandstone formation · South Rumaila oil field

## Introduction

Spatial lithofacies modeling is a very important step in reservoir characterization because it accurately reflects the stratigraphic reservoir structure and provides clear insights into how the reservoir is subdivided through flow unit zonation. A lithofacies model is beneficial because it helps individuals understand the description of different depositional environments in addition to capturing all of the heterogeneity levels and scales which are integrated into the reservoir flow model (Mikes and Geel 2006; Walker 1992). The facies model can also serve as a guide to predict reservoir properties in different locations with the same depositional environment by controlling the reservoir heterogeneities and fluid flow characteristics (Walker 1992). The type and architecture of the geological facies and their related petrophysical data distribution are crucial issues with direct influences on reservoir heterogeneities, fluid flow performance prediction, field development, and economic evaluation (White and Royer 2003). The process of integrating all available geological information into the numerical reservoir simulation in terms of 3D facies distribution is called facies modeling (Walker 1992). For accurate facies distribution, it is necessary to efficiently integrate the different scales of data to capture the reservoir heterogeneity and transfer it into the reservoir model. The most recent

✉ Watheq J. Al-Mudhafar  
wmoham4@lsu.edu

<sup>1</sup> Louisiana State University, 105 Old Forestry Building, Baton Rouge, LA 70808, USA

<sup>2</sup> South Oil Company, Basrah, Iraq

methods that have been used to quantify the facies and petrophysical properties involve deterministic (estimation) and stochastic (simulation) approaches (Journel 1989, 1990; Journel and Alabert 1990; Journel and Gomez-Hernandez 1993; Overeem 2008).

Several methods have been used for facies modeling including variogram-based methods, object-based modeling, and multiple-point geostatistics (Liu et al. 2004; Zhang 2008). The most commonly performed geostatistical models are pixel-based methods. Pixel-based models are used for stochastic modeling of either discrete distribution variables such as facies or continuous distribution variables such as porosity or permeability. More specifically, pixel-based models encompass sequential indicator simulation for facies and sequential Gaussian simulation for petrophysical properties.

The pixel-based model is used to build the categorical image, pixel by pixel, considering nonparametric condition distribution. The pixel-based model, sometimes referred to as two-point statistics, depends on the variogram to address and model the variation between any two spatial points from the available data (Caers and Zhang 2004; Deutsch and Journel 1998; Liu et al. 2004; Zhang 2008). Although it is simple and requires few parameters, the pixel (variogram)-based modeling has some limitations including its inability to capture complex geological structures such as channel shapes, thickness, and sinuosity. For instance, it is unable to capture models with many different geological formations with the same variogram but different architectures (Caers and Zhang 2004).

Sequential indicator simulation (SISIM) is used to build a conditional probability density function of nonparametric properties, such as rock type, by considering binary simulation (Caers 2000; Deutsch and Journel 1998). Once the continuous variable is transformed into a number of indicator variables, one for each class, each of the indicator variables is spatially modeled using any of the variogram or covariance functions. In SISIM, the facies data are encoded into binary values (0, 1) controlled by giving threshold values. Then, spatial distribution is characterized by the indicator variograms in order to generate alternative equiprobable stochastic reservoir images. The binary encoding could also be adopted for the main facies characterization such as sand and shale (Journel and Gomez-Hernandez 1993). Moreover, the facies can be encoded as binary variables given a specific location to represent different rock types, such as one for sand channels and zero for lobe, in a complex turbiditic reservoir (Alabert and Massonnat 1990). Additionally, SISIM can predict the facies distribution in inter-well regions through log signatures to characterize major log associations in non-cored wells and provide conditional data for the stochastic facies distribution.

To capture the marine to fluvial transition, the SISIM has been modified to incorporate a vertical trend in the mean proportion of each of the major facies associations (Begg et al. 1996).

Sequential indicator simulation has been widely accepted in many different reservoir characterization studies. Specifically, SISIM has been successfully used for lithofacies modeling to characterize flow barriers and/or flow paths and fractures in sandstone formations (Journel and Alabert 1990), complex turbiditic reservoir (Alabert and Massonnat 1990), and sand-shale reservoirs (Massonnat et al. 1992).

Different data sources and scales, such as well data, seismic, and geological interpretation, can be integrated to build the facies model through SISIM and Co-SISIM (Journel and Alabert 1990). Sequential indicator simulation has also been widely described in many other studies (Alabert and Modot 1992; Goovaerts 1997; Seifert and Jensen 1999; Srivastava 1994).

Consequently, the sequential indicator simulation was adopted in this paper to reconstruct the 3D lithofacies model of tidal depositional environment of the upper sandstone member/Zubair formation in the south Rumaila oil field. The approximate reconstruction of the lithofacies based on the depositional environment description leads to preserve the reservoir heterogeneity because petrophysical properties' permeability and porosity are later distributed given each lithotype, not as a function of the entire reservoir of one approximate facies type.

## Field description

### Introduction

Discovered in October 1953 by Basrah Petroleum Company, the Rumaila oil field is located in southern Iraq about 50 km west of Basrah city and about 30 km to the west of the Zubair oil field (Al-Ansari 1993). It is about 100 km long, 12 to 14 km wide, and more than 3 km below sea level. Dip angles on the flanks do not exceed 3°, but are about 1° in the crest. Faults are not indicated in all layers of the Rumaila field (Al-Ansari 1993). The geographical location of south Rumaila oil field is shown in Fig. 1. The area remarked in Fig. 1 contains the most geologic and reservoir data and is the main sector in the south Rumaila oil field. This sector contains 40 producers and 20 injectors (Mohammed et al. 2010). However, discrete lithofacies distributions of the wells in this sector are only provided for 19 wells. These wells are in all areas of the reservoir which enables efficient 3D lithofacies modeling. Figure 2 illustrates the current well locations in the south Rumaila oil field.

### Geological description

The south Rumaila oil field is composed of many oil-producing reservoirs. Zubair is one of the oil reservoirs that are represented by the Late Berriasian-Albian cycle and its

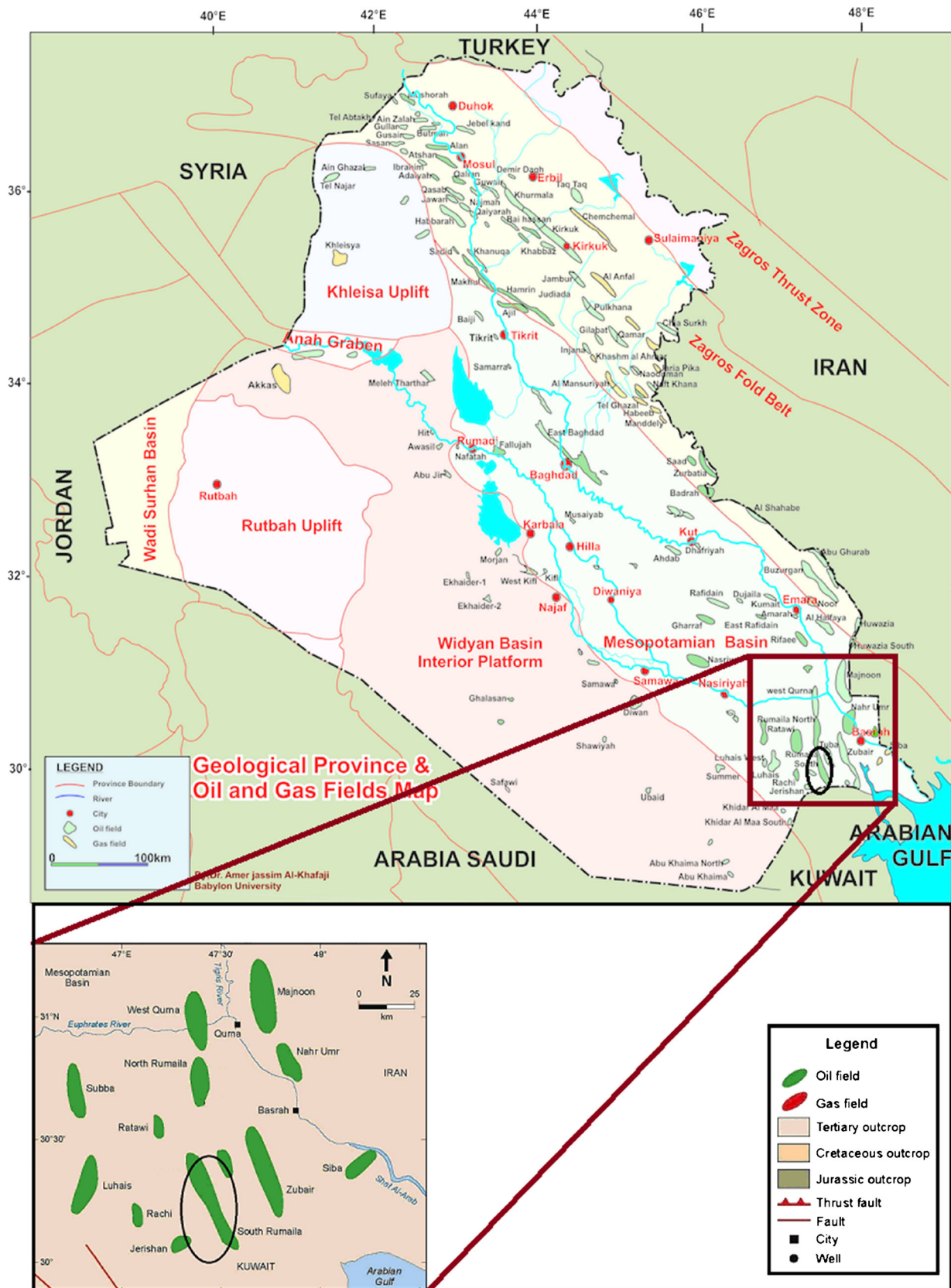


Fig. 1 Geographical location of oil and gas fields in Iraq, including south Rumaila oil field (modified from Al-Ameri et al. 2009)

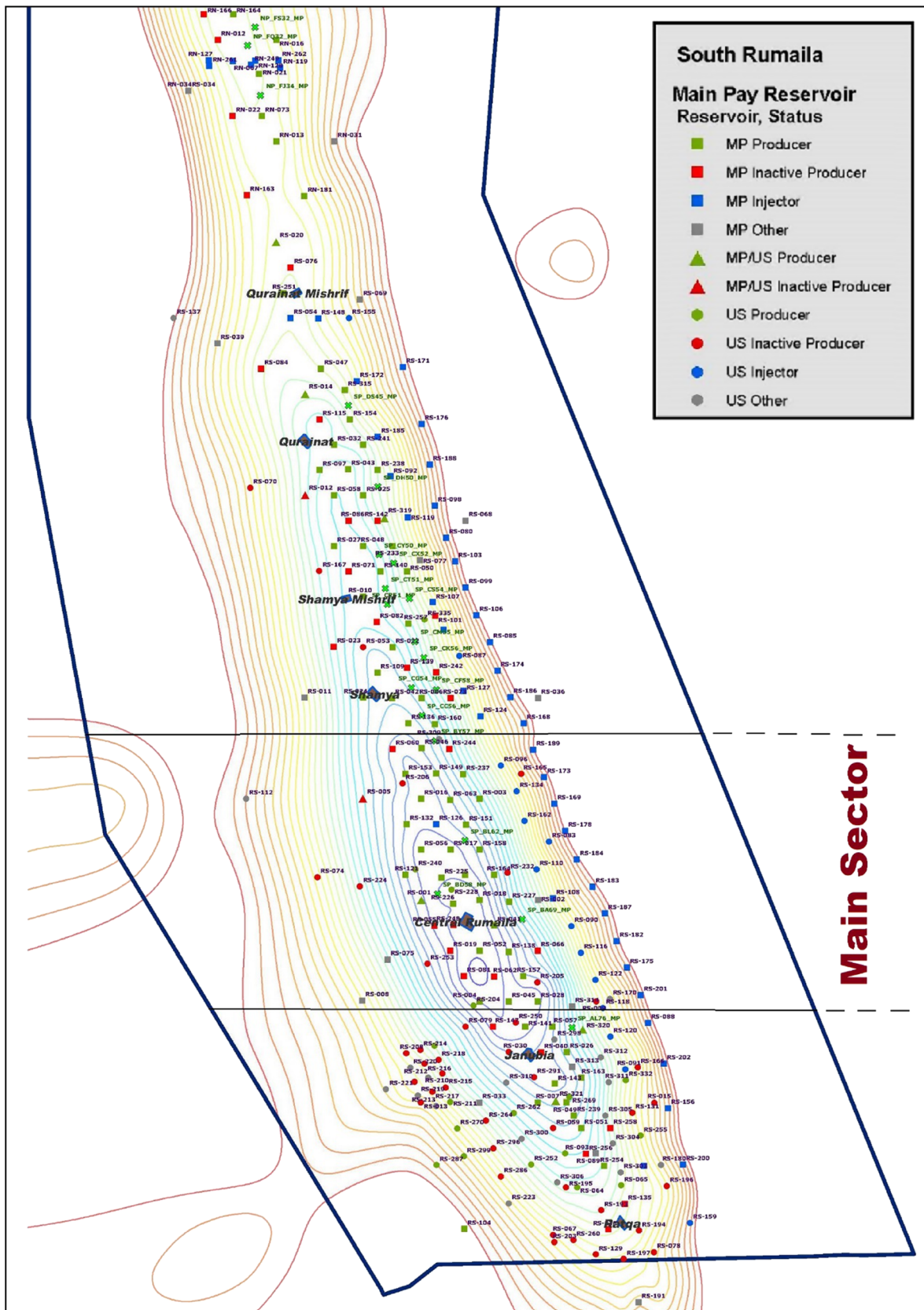


Fig. 2 Current well locations for the sector under study in the main pay/south Rumaila oil field

sediments, which belongs to the Lower Cretaceous age. The Zubair formation is rich in organic deposition and accumulation of sedimentary matter (Al-Obaidi 2010). The thickness of the Zubair formation ranges between 280 and 400 m with levels increasing towards northeast end of the field (Al-Obaidi 2009). Based on the sand to shale ratio, the Zubair formation encompasses five members. These members named from top to bottom are as follows: upper shale member, upper sandstone member, middle shale member, lower sand

member, and lower shale member. The upper sandstone member of the Zubair formation is the main pay zone of south Rumaila oil field (Mikes and Geel 2006). The main pay comprises of five dominated sandstone units, separated by two discontinuous shale units (C and K), as shown in Fig. 3. The shale units act as barriers impeding vertical migration of the reservoir fluids; however, in some areas, they are not as prominent. The reservoir and shale units have been denoted from top to bottom as AB, C, DJ1, DJ2, K, LN1, and LN2

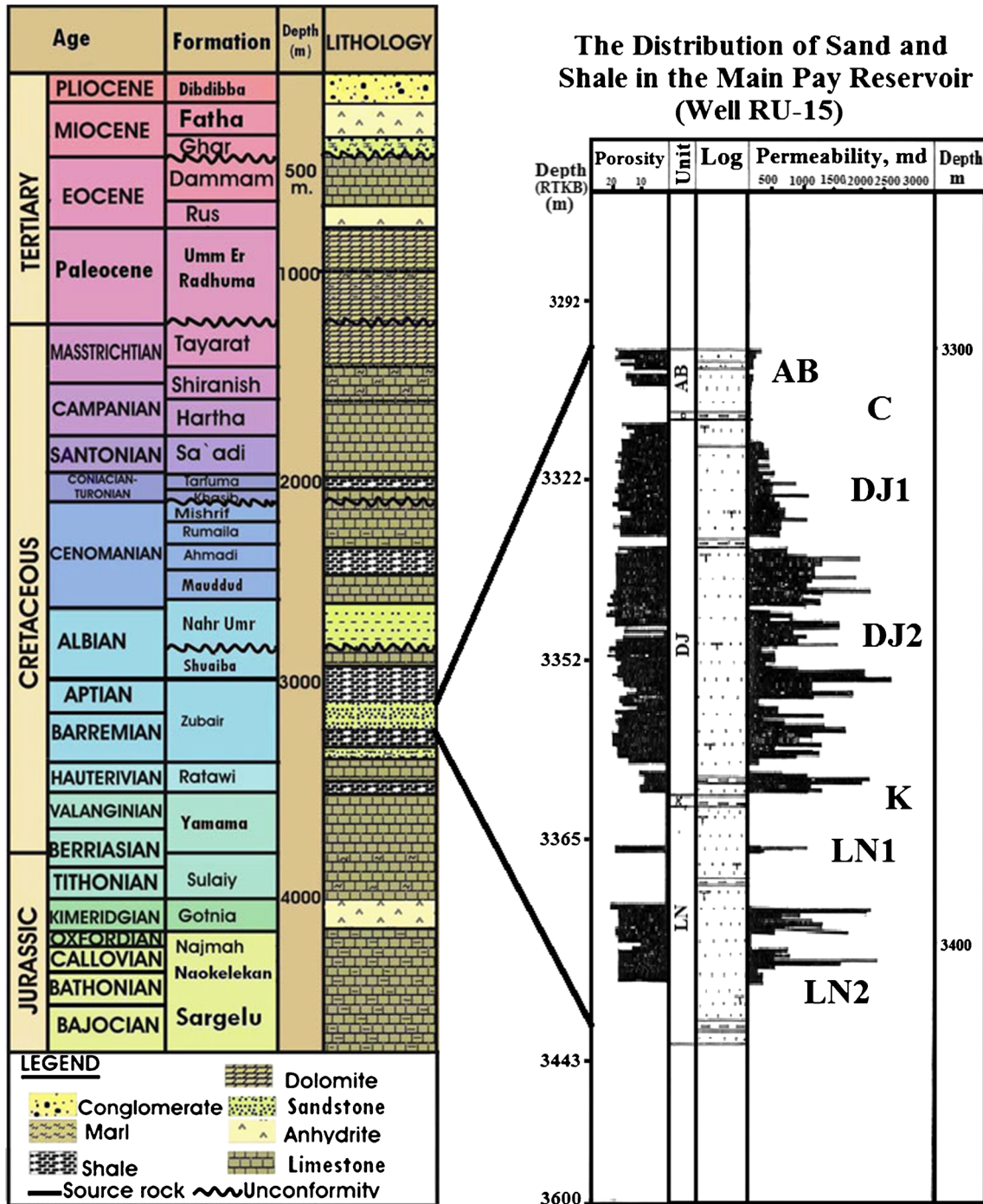


Fig. 3 Geological lithology column of the formations in south Rumaila oil field (modified from Mohammed et al. 2010)

(Mohammed et al. 2010). The geological column for the entire reservoir’s zones in the Rumaila oil field is shown in Fig. 3.

**Depositional environment**

The Zubair formation is part of the Lower Cretaceous sequence age. It is located between two dolomite-limestone and shale formations that are named Shuaiba and Ratawi, respectively. The Zubair formation encompasses mainly sandstone with some inter-bedded shale zones (Al-Muhailan et al. 2013). Figure 4 shows the stratigraphic column with vertical lithology description and well log indications for all the zones in the south Rumaila oil field.

Overall, the Zubair formation was deposited through deltaic, estuarine, and fluvial environments (Harris et al. 2012). The upper shale member, which is located above the upper sandstone member, was deposited in a wave/shoreface and offshore-dominated environment resulting in sand channels that extend east-west across the anticline (Al-Muhailan et al. 2013). The upper and middle sandstone members were deposited in a tidal/estuarine environment in which the sand channels are stacked and continuous everywhere across the formation. The lower sandstone member was deposited in a fluvial/mouth bar-dominated environment. The analyses of core samples have indicated coarsening upward black claystones at the

base of the lower part of the upper sandstone member overlain by bioturbated very fine-grained sandstones, which in turn are overlain by fine-grained, trough cross-bedded sandstones. The same events took place at the middle sandstone member (Harris et al. 2012). The core sedimentology, palynofacies observations, and biostratigraphic analyses indicate both marine and terrestrial microflora confirm a marginal marine gross depositional environment. On the other hand, the palynology studies have proven the succession of the very fine- and fine-grain sandstones (Kitching et al. 2013).

Another study stated that the main pay was a fluvially dominated, sand-rich deltaic environment (Wells et al. 2013). The study likewise highlights the phased advance and retreat of a river-dominated and tidally influenced delta system. Additionally, the observation of cyclic bundles of the thin forest shale laminae confirms the influence of tides. Marine flooding surfaces were also observed and usually succeeded by prodelta shales that affect the vertical connectivity in the formation. Nevertheless, most of the effective reservoir rocks are of a high quality in lateral and vertical amalgamates. Excluding the shale distribution, the entire sand distribution tends to be heterogeneous through rapid lateral and vertical variations (Al Naqib 1967). In the southern part of the field, core analysis indicates fine- to medium-grained cross-bedded sandstones, which were mainly deposited in lower delta plain

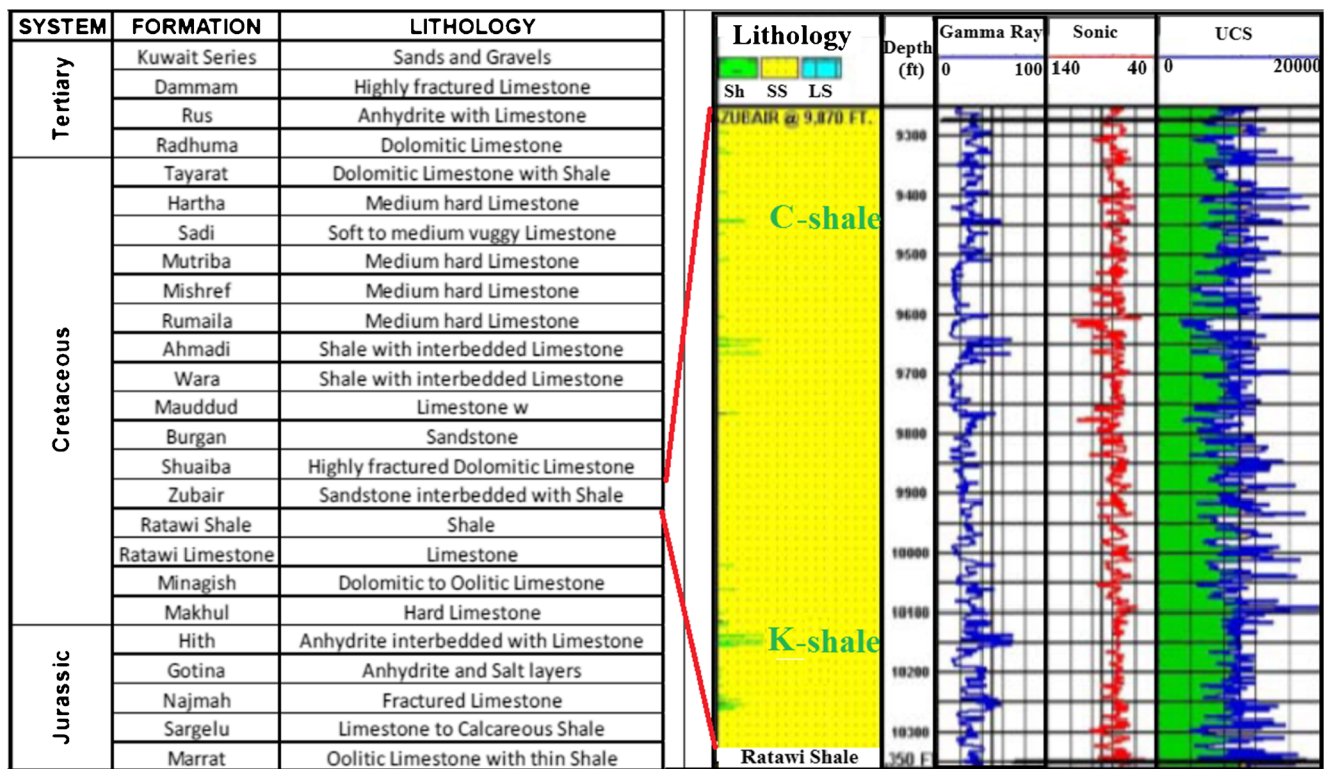


Fig. 4 Stratigraphic column of Rumaila field with lithology (left). Lithology and well log data for Zubair formation only (right) (modified from Al-Muhailan et al. 2013)

distributed channels. However, the grain sizes tend to decrease in mixed sand and shale deposits that were preserved in the northern area of the field (Wells et al. 2013).

Since there are contradictions between the various facies studies on the upper sandstone member, the 3D lithofacies modeling in this study was conducted considering the description provided by Harris et al. (2012) which stated the tidal/estuarine depositional environment of the upper sandstone member.

### Geostatistical reservoir modeling

Isaaks and Srivastava (1989) stated that “Geostatistics offers a way of describing the spatial continuity of natural phenomena and provides adaptations of classical regression techniques to take advantage of this continuity.” Geostatistics integrates mathematical concepts, computer technology, and stochastic modeling to generate multiple equiprobable realizations that keep the reservoir heterogeneity by honoring all the available data (Caers and Zhang 2004; Deutsch and Journel 1998; Journel 1990; Liu et al. 2004). These alternative stochastic images (realizations) are created through conditional stochastic simulation with the ability to reproduce extreme values, such as high-permeability channels and low-permeability barriers, in order to quantify the geological spatial uncertainty (Caers 2005). The geological uncertainties occur due to incomplete information regarding the modeled phenomenon (Goovaerts 1997; Pyrcz and Deutsch 2014). Most geostatistical reservoir characterization models are variogram-based algorithms such as sequential indicator simulation for facies modeling and sequential Gaussian simulation for continuous petrophysical parameters.

### Variogram-based algorithms

Variogram-based geostatistics, also called two-point statistics or traditional two-point geostatistics, adopt variogram models to describe the variation between any two spatial data locations (Gringarten and Deutsch 1999; Liu et al. 2004; Zhang 2008; Deutsch and Journel 1998).

The variogram describes the geometry and continuity of reservoir properties and has direct impact on the flow behavior. The variogram can be defined as the measure of dissimilarity between known and unknown data as the distance increases and mathematically is the expected squared difference between two data values separated by a distance vector  $h$  (Gringarten and Deutsch 1999).

$$2\gamma(h) = E[Y(u) - Y(u + h)]^2 \tag{1}$$

where  $h$  represents the spatial lag distance between two points,  $\gamma(h)$  refers to the variance between two points with distance  $h$ ,  $Y(u)$  refers to the variance of parameter at point  $u$ , and  $Y(u + h)$  represents the variance of parameter at point  $u + h$ . The variogram terminology includes sill (the plateau that variogram reaches the range); range (the distance at which the variogram no longer increases with distance increases); and nugget (measurement error when distance is zero). These parameters are represented in Fig. 5.

$$\gamma(h) = var(z) - cov(h) \tag{2}$$

$$Dissimilarity(h) = Sill - Similarity(h)$$

where  $var(z)$  refers to the sill or variation of parameter  $z$  and  $cov(h)$  represents the covariance or similarity between data in distance  $h$ . Simple kriging is then used for spatial data distribution based on best variogram fit.

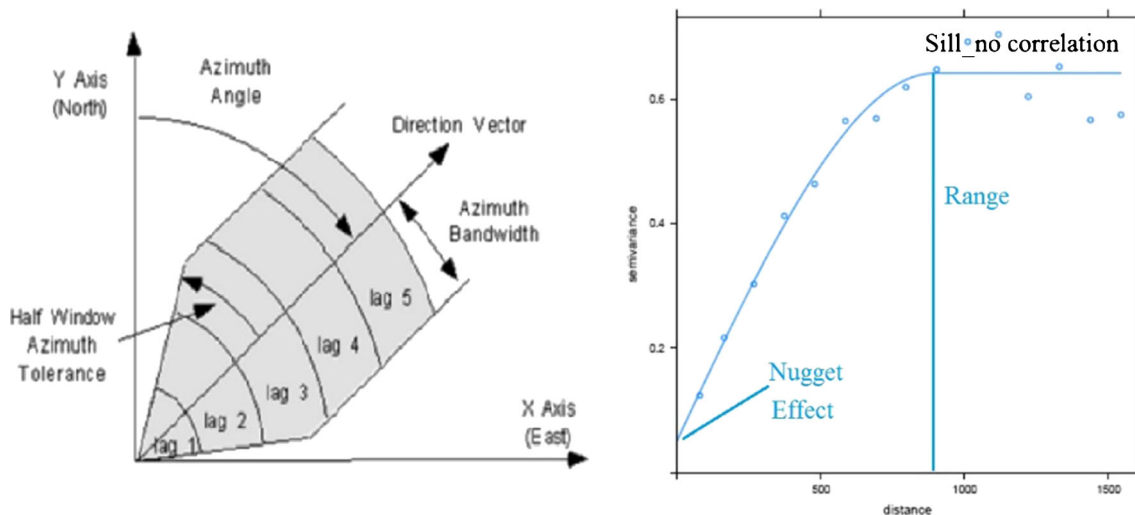


Fig. 5 Variogram structure

$K$  is the covariance matrix between the known data.

$$K = \begin{pmatrix} cov(Z_1, Z_1) & cov(Z_1, Z_2) & \cdots & cov(Z_1, Z_n) \\ cov(Z_2, Z_1) & cov(Z_2, Z_2) & \cdots & cov(Z_2, Z_n) \\ \vdots & \vdots & \ddots & \vdots \\ cov(Z_n, Z_1) & cov(Z_n, Z_2) & \cdots & cov(Z_n, Z_n) \end{pmatrix} \quad (3)$$

where  $K$  is the covariance matrix between known data in variogram,  $k$  is the covariance vector between the known and unknown data, and  $\lambda$  is the kriging weights.

$$k = \begin{pmatrix} cov(Z_1, Z_0) \\ cov(Z_2, Z_0) \\ \vdots \\ cov(Z_n, Z_0) \end{pmatrix} \sim \lambda = \begin{pmatrix} \lambda_1 \\ \lambda_2 \\ \vdots \\ \lambda_n \end{pmatrix} \quad (4)$$

where  $k$  is the covariance matrix between known and unknown data in variogram, and  $\lambda$  is the kriging weights in variogram. The final formula of simple kriging is

$$z_0 = \sum_{i=1}^n \lambda_i z_i \quad (5)$$

where  $z_0$  is the predicted value of parameter  $z$  in simple kriging and

$$\sum_{i=1}^n \lambda_i = 1.$$

The variogram-based conditional simulation algorithms include sequential Gaussian simulation for continuous variables and sequential indicator simulation for categorical variables (lithofacies). The sequential indicator simulation (SISIM) was adopted in this study for the 3D lithofacies modeling of the upper sandstone member of south Rumaila oil field, as it is described below.

### Sequential indicator simulation

The most common geostatistical facies modeling is SISIM which is designed for modeling the spatial distribution of facies based on the indicator variogram (Journel and Alabert 1990; Massonnat et al. 1992). The indicator variogram is used to build up a discrete cumulative density function (CDF) for the individual facies types and the node is assigned a lithotype,  $k$ , selected at random from this discrete CDF (Journel and Gomez-Hernandez 1993). After encoding facies into elementary samples 0, 1 given threshold values, the indicator variogram then can be formulated as

$$I(Z_k; x) = \begin{cases} 0 & \text{if } Z(x) > Z_k \\ 1 & \text{if } Z(x) \leq Z_k \end{cases} \quad (6)$$

where  $I(Z_k; x)$  is the indicator random variable that is associated with random function  $Z(x)$  for a threshold value  $Z_k$ . The expected value of the indicator random variable  $I(Z_k; x)$  is

equal to the cumulative probability  $Pr\{Z(x) < Z_k\}$  as shown below:

$$E(I(Z_k; x)) = 0 \times Pr\{Z(x) > Z_k\} + 1 \times Pr\{Z(x) \leq Z_k\} \quad (7)$$

$$E(I(Z_k; x)) = Pr\{Z(x) < Z_k\} \quad (8)$$

where  $Pr\{Z(x) < Z_k\}$  represents the cumulative probability in SISIM. According to the logic described about SISIM, the SISIM is considered as a nonparametric sequential simulation (Caers 2000). The main SISIM procedural steps for the facies spatial modeling after establishing the grid network and coordinate system are demonstrated below (Goovaerts 1997; Journel and Gomez-Hernandez 1993; Pyrcz and Deutsch 2014):

1. Create the indicator variogram for each lag distance based on the indicator lithofacies.

$$\gamma(h) = \frac{1}{2N_h} \sum_{i=1}^{N_h} (\text{facies}_{(h+i)} - \text{facies}_{(h)})^2 \quad (9)$$

where  $N_h$  is the number of points included in indicator variogram. The prior distribution function represents the density distribution of the facies and it is calculated as

$$F(z_i) = \sum_{j=1}^{i-1} P(z_j) \quad (10)$$

where  $F(z_i)$  represents the prior distribution function of facies and  $P(z_j)$  refers to the density distribution of the facies.

2. Select randomly all the un-sampled locations to be simulated.
3. Consider the indicator kriging to estimate the probability that un-sampled location prevails given the indicator values at the surrounding locations.
4. Randomly specify the indicator values to be either 0 or 1.
5. After adding the simulated indicator value to the sampled data group, repeat the procedure for the remaining un-sampled locations.
6. Repeat this procedure for all the realizations.

The SISIM was adopted to reconstruct the 3D lithofacies modeling of the upper sandstone member of south Rumaila oil field. Since the azimuth direction of the shoreline is not clearly identified in the literature, the SISIM was attained to reconstruct the lithofacies model in four azimuth directions. These four different azimuths cover the entire range of the actual depositional flowing. However, the sea is located in the south-east and the shoreline should be closer to the azimuth direction of 135°. As an assumption, the dip angle was set to be zero as a default value and minor range was set to be 500 for all the four azimuth directions. However, the major ranges were different given each lithotype and azimuth. The values of major range were selected to achieve the best fitting of the indicator



variogram that covers the distance-based correlation between where the sample points in the reservoir. The best values of major ranges control the channel continuity (stationary) in the tidal depositional environment.

### Results and discussion

Among 60 wells in the main pay of the south Rumaila oil field, only 19 wells have the vertical discrete lithofacies distribution of sand, shaly sand, and shale. The discrete lithofacies measurements have been first obtained from a core measurement report from a well in south Rumaila oil field. Then, the distributions for the 19 wells have been predicted by the support vector machine algorithm in previous studies (Al-Mudhafar 2015, 2017). Figure 6 depicts samples of the discrete lithofacies distributions (sand, shaly sand, and shale) for some wells in south Rumaila oil field. Figure 7 shows all

wells that have lithofacies distributions with their actual locations in the reservoir.

The first step in building the 3D property model is to construct the structural model that includes grid structure and horizon modeling. The grid structure involves setting the grid system for the reservoir to be considered for all the upcoming geological and reservoir modeling. The chosen dimensions of each grid in the orthogonal corner gridding were 50 m × 50 m and the number of grids (cells) in *I* direction was 210, and in *J* direction was 202 grids. In the horizontal modeling, the main reservoir has five zones. To capture a more realistic geological structure, the zones were subdivided into 45 layers to have approximately 2 m depth for each layer. Thus, the number of grids in *K* direction was 45 grids. The final geostatistical model has 1,908,900 total number of grids for all the layers. Figure 8 shows the structure gridded surface for the reservoir including the layering structure.

For the geostatistical lithofacies modeling, the sequential indicator simulation was adopted to reconstruct a 3D

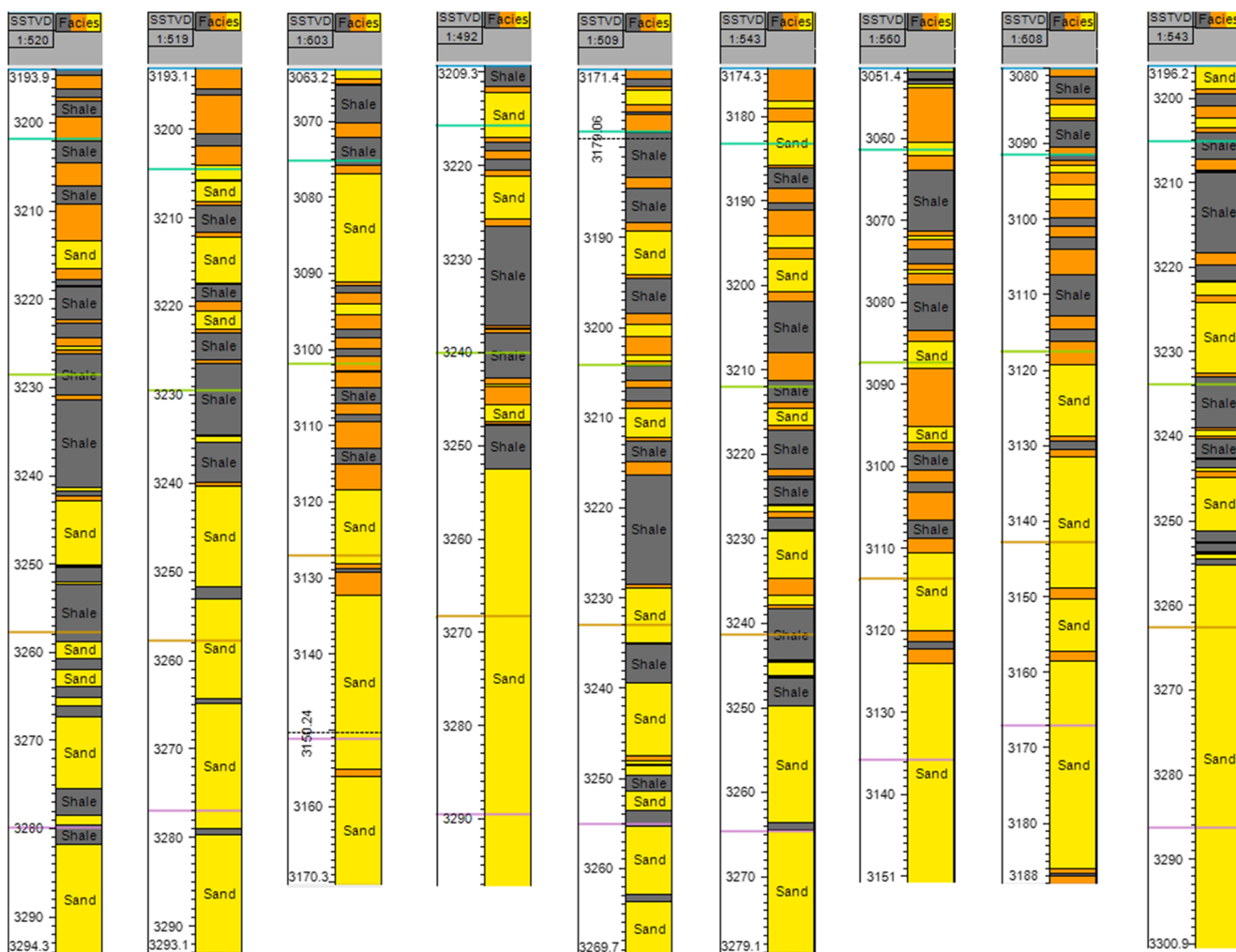
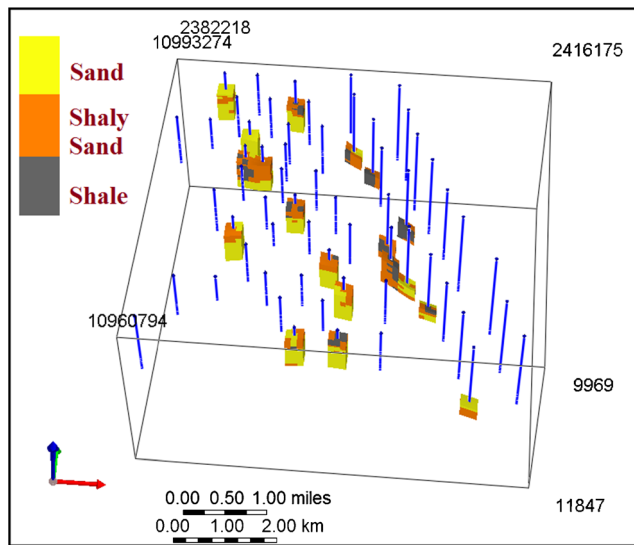


Fig. 6 The vertical discrete lithofacies distributions for some wells in south Rumaila oil field



**Fig. 7** Well locations and available measured discrete well lithofacies distributions

lithofacies distribution for the sector of south Rumaila oil field/main pay. The well lithofacies distributions were upscaled, given each layer prior to starting the 3D geostatistical lithofacies modeling. The main steps for the implementation procedure of sequential indicator simulation are outlined below:

1. Upscale well log data
2. Construct and fit indicator variogram
3. Random seed number
4. Frequency distribution of upscaled data points

The variogram-based stochastic simulation has been used to identify the spatial structure of the main pay/Zubair formation in south Rumaila oil reservoir. The variogram is a function that describes the correlation between the values of sand, shaly sand,

and shale of points in space, depending on the distance between them. The variogram is constructed based on the assumption that the correlation function between these values depends only on the relative position of measured points not on their locations in space. Using the experimental data and given the suspicions about the existence of differences in the spatial structure, the calculated experimental directional variograms for sand, shaly sand, and shale are constructed in four different azimuth directions. More specifically, the sequential indicator simulation considers the indicator variogram to obtain the spatial correlation of each lithotype in four different angles: 0° (horizontal), 45°, 90° (vertical), and 135°. The constructed and modeled indicator variograms for all the facies types given each direction are depicted in Fig. 9.

In Fig. 9, the three top-left plots represent the indicator variogram for the sand, shaly sand, and shale in horizontal direction. The three top-right plots represent the indicator variogram for the sand, shaly sand, and shale in 45° direction. The three bottom-left plots represent the indicator variogram for the sand, shaly sand, and shale in vertical direction. The three bottom-right plots represent the indicator variogram for the sand, shaly sand, and shale in 135° direction.

The spatial correlation of each lithotype was accomplished versus lag distance in those azimuth directions. Choosing the four main azimuth directions is to test and capture the different spatial correlations in horizontal direction for heterogeneity and vertical direction for anisotropy. The number of lags in all the cases was 20, the average range of major directions was 2000 m, and the bandwidth of the search cone was around 2000 m. These parameters were chosen to capture all possible wells with sufficient data.

After construction and fitting the empirical indicator variograms, the standard covariance parameters, sill, nugget, and range, were collected to be used in 3D spatial distribution algorithm (solving the kriging equation). The spherical modeling

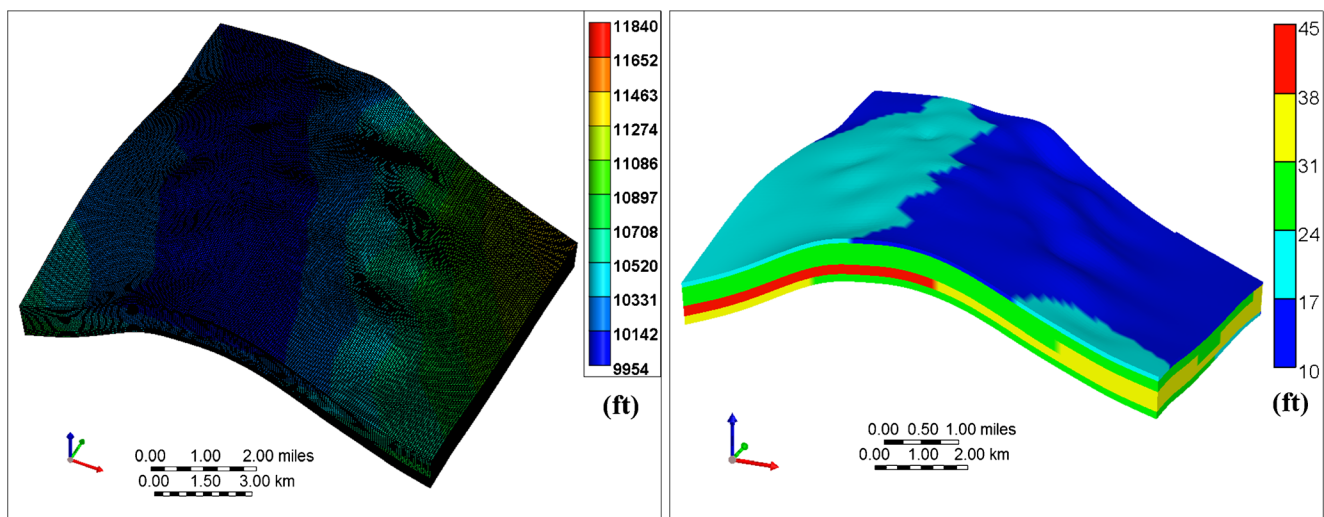


**Fig. 8** Gridding system (left). Zone's layer thickness for the main pay/south Rumaila field (right)

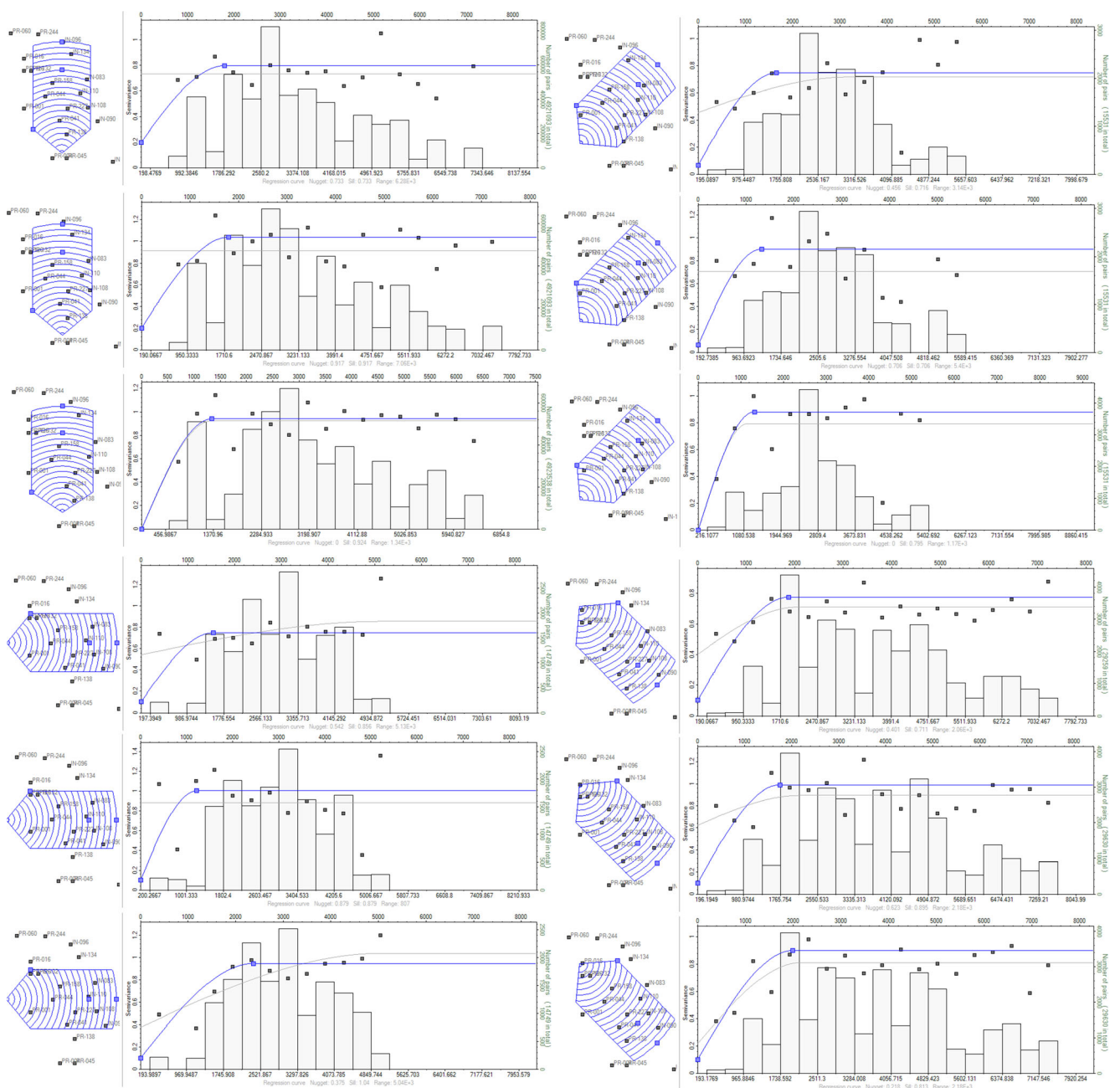


**Fig. 9** Twelve indicator major variograms for the three facies in four azimuth directions: the three (*top-left*) variograms for the 0° (horizontal) azimuth direction. The three (*top-right*) variograms for the 45° azimuth

direction. The three (*bottom-left*) variograms for the 90° (vertical) azimuth direction. The three (*bottom-right*) variograms for the 135° azimuth direction

is the best fit for all the indicator variograms for all the lithotypes in the four azimuth directions. Table 1 illustrates the indicator variogram parameters for the lithofacies modeling in the four azimuth directions.

The variogram results for sand in a horizontal direction indicate that there is nugget effect, i.e., strong variability of the content with lack of correlation between the data. This may be due to the uncertainty of measurement or variability of data on a smaller scale. Additionally, the results of shaly

sand variograms turned out a poor representative. In the horizontal direction and at an angle of 45° and 90°, there is an observed nugget effect, and at an angle of 135°, there is large nugget of 0.623, sill of 0.895, and the range of 2180 ft, which indicates a weak correlation of shaly sand. However, the variogram results for shale were very good in all azimuth directions. The nugget is completely absent in the horizontal direction and at an angle of 45°, indicating the properly selected scale and quality of experimental data. Moreover, the

**Table 1** Indicator variogram parameters for all the lithofacies in the four azimuth directions

Facies	Range			Azimuth	Nugget	Variogram type
	Major	Minor	Range			
Sand	1800	500	100	0	0.197	Spherical
Shaly sand	1795	500	100	0	0.201	Spherical
Shale	1340	500	100	0	0.00	Spherical
Sand	1658	500	100	45	0.067	Spherical
Shaly sand	1326	500	100	45	0.063	Spherical
Shale	1320	500	100	45	0.0	Spherical
Sand	1550	500	100	90	0.1	Spherical
Shaly sand	1215	500	100	90	0.1	Spherical
Shale	2376	500	100	90	0.1	Spherical
Sand	1872	500	100	135	0.1	Spherical
Shaly sand	1753	500	100	135	0.1	Spherical
Shale	1997	500	100	135	0.1	Spherical

nugget ranges from 0.218 to 0.375 at 90° and 135° degrees. For all lithotypes, the range of the correlated data is 1170–5040 ft.

The outputs of indicator variogram fit such as sill, nugget, and range are necessary for the 3D facies modeling through the sequential indicator simulation. To honor all the data, histogram, variogram, and correct smoothing, the sequential indicator simulation was adopted for 3D facies modeling rather than the indicator kriging, which does not represent more than facies plotting (deterministic). Figure 10 shows the 3D lithofacies modeling given the four variogram azimuth directions for the search cone, which was set for the indicator variogram. The top-left figure represents the lithofacies in 0°, the top-right represents the lithofacies in 45°, the bottom-left represents the lithofacies in 90°, and the bottom-right represents the lithofacies in 135°.

It can be seen in Fig. 10 that this reservoir consists mainly of sandstone with some inter-bedded shale zones, as mentioned before. A decrease mixed sand and shale deposits are preserved in the northern area of the field as mentioned before (the angle of 135°). In addition, the most effective reservoir rocks of high quality, with less shaly sand, have inhomogeneous distribution with rapid vertical and lateral variations. Furthermore, the entire sand distribution tends to be heterogeneous through rapid lateral and vertical variations.

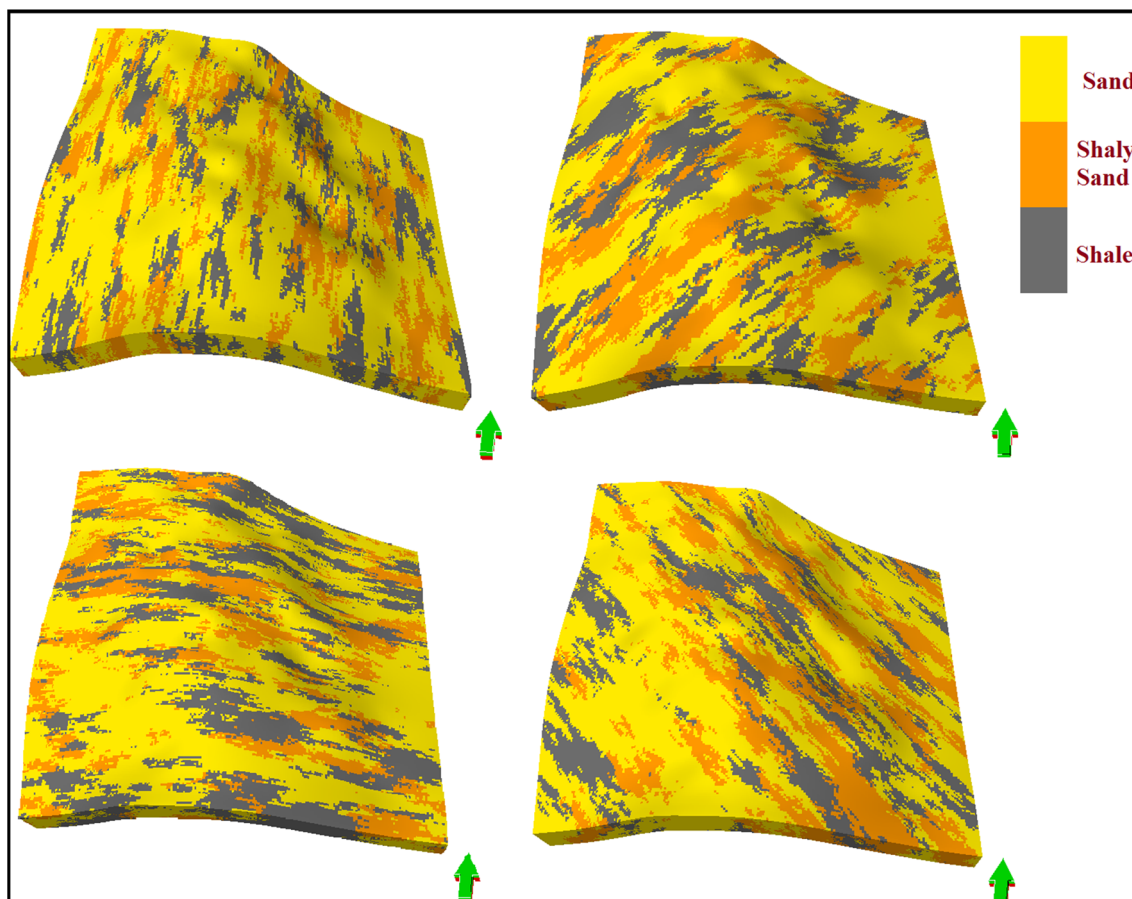


**Fig. 10** 3D variogram-based geostatistical lithofacies distributions in the four different azimuth directions for the main pay in south Rumaila oil field. The four models represent the lithofacies given four variogram azimuth directions (0°, 45°, 90°, and 135°) by using the sequential

indicator simulation (SISIM). The lithofacies are sand, shaly sand, and shale. The variograms have been created given each lithotype in the four azimuth directions

In order to judge the accuracy of the resulting 3D facies modeling for the main pay/south Rumaila field, one should consider the depositional environment of tidal/estuarine in which the sand channels are stacked and continuous everywhere across the formation. The resulting lithofacies modeling provides an approximate description of that tidal depositional environment in all the four direction models. Since the shoreline direction of south Rumaila field is located at the southeast direction, the lithofacies model of 135° tends to be the most accurate depositional description that preserves the reservoir heterogeneity and captures the most realistic geological environment.

## Summary and conclusions

To capture the most realistic geological model and to preserve the reservoir heterogeneity, the geostatistical modeling of Sequential Indicator Simulation (SISIM) was adopted for 3D lithofacies reconstruction of the upper sandstone member/Zubair formation in south Rumaila field, located in Iraq. The SISIM algorithm was implemented to capture the tidal/estuarine depositional environment of the reservoir. The SISIM was adopted on the reservoir in a high resolution of approximately two million gridding systems. Four different directions of the indicator variograms were estimated and modeled for the lithofacies data to create the 3D lithofacies models given these four azimuth directions.

The indicator variograms were necessary to link and quantify correlation between geological variations through modeling the similarity between discrete lithofacies with the spatial lag distance. Specifically, indicator variogram modeling is a way to incorporate the geological knowledge into reservoir characterization process in order to reduce the uncertainty of spatial modeling. The resulting 3D lithofacies modeling encompasses mainly of sandstone with some inter-bedded shale and shaly sand zones that match the tidal/estuarine depositional system, which has been described in the literature. Specifically, the shape of the resulting 3D modeling through SISIM has clearly indicated the tidal/estuarine-dominated and sand-rich environment for the upper sandstone formation. According to the southeast shoreline direction of south Rumaila field, the lithofacies model of 135° describes the most realistic depositional environment that captures the reservoir complexity and heterogeneity.

The resulting 3D lithofacies model can be then used as basis for the petrophysical property modeling given each lithotype. That leads to preserve the reservoir heterogeneity.

**Acknowledgements** The author would like to present his thanks and appreciation to the Institute of International Education for granting the Fulbright Science and Technology Awards that has funded the PhD

Research. Thanks also go to Schlumberger Co. for granting the university a free version of Petrel Software.

## References

- Al Naqib KM (1967) Geology of the Arabian peninsula southwestern Iraq. Paper 560-G, U.S. Geological Survey Professional. United States Government Printing Office, Washington
- Alabert FG, Massonnat GJ (1990) Heterogeneity in a complex turbiditic reservoir: stochastic modelling of facies and petrophysical variability. SPE-20604-MS paper presented at the SPE Annual Technical Conference and Exhibition, New Orleans, Louisiana, 23–26 September 1990
- Alabert FG, Modot V (1992) Stochastic models of reservoir heterogeneity: impact on connectivity and average permeabilities. SPE-24893-MS paper presented at the SPE annual technical conference and exhibition, Washington, D.C., 4–7 October 1992
- Al-Ameri TK, Al-Khafaji AJ, Zumberge J (2009) Petroleum system analysis of the Mishrif reservoir in the Ratawi, Zubair, North and South Rumaila oil fields, southern Iraq. *GeoArabia* 14:91–108
- Al-Ansari R (1993) The petroleum geology of the upper sandstone member of the Zubair formation in the Rumaila south. Geological Study, Ministry of Oil, Baghdad
- Al-Mudhafar WJ (2015) Integrating component analysis & classification techniques for comparative prediction of continuous & discrete lithofacies distributions. Offshore technology conference. doi:10.4043/25806-MS
- Al-Mudhafar WJ (2017) Integrating kernel support vector machines for efficient rock facies classification in the main pay of Zubair formation in South Rumaila oil field, Iraq. *Model Earth Syst Environ* 3:12. doi:10.1007/s40808-017-0277-0
- Al-Muhailan M, Hussain I, Maliekkal H, Ghoneim O, Nair P, Fayed M (2013) New HTHP cutter technology coupled with FEA-based bit selection system improves rop by 60% in abrasive Zubair formation. IPTC-17122, paper presented at the International Petroleum Technology Conference, Beijing, China
- Al-Obaidi RY (2009) Identification of Palynozones and age evaluation of Zubair Formation, Southern Iraq. *Journal of Al-Nahrain University* 12(3):16–22
- Al-Obaidi RY (2010) Determination of Palynofades to assess depositional environments and hydrocarbons potential, Lower Cretaceous, Zubair Formation South Iraq. *Journal of College of Education* 5: 163–174
- Begg SH, Kay A, Gustason ER, Angert PF (1996) Characterization of a complex fluvial-deltaic reservoir for simulation. *SPE Form Eval* 11(03):47–154
- Caers J (2000) Direct sequential indicator simulation. In the 6th International Geostatistics Congress, South Africa, 10–14 April 2000
- Caers J (2005) Petroleum geostatistics. Society of Petroleum Engineers, Richardson
- Caers J, Zhang T (2004) Multiple-point geostatistics: a quantitative vehicle for integrating geologic analogs into multiple reservoir models. *AAPG Mem* 80:383394
- Deutsch CV, Journel AG (1998) *GSLIB. Geostatistical software library and user's guide*, New York
- Goovaerts P (1997) *Geostatistics for natural resources evaluation*. Oxford University Press, New York
- Gringarten E, Deutsch CV (1999) Methodology for variogram interpretation and modeling for improved reservoir characterization. In SPE annual technical conference
- Harris GD, Wellner RW, Catterall V, Kairo S, Liu C, Chen Y (2012) Stratigraphy and depositional environment of the upper Zubair

- sandstone (Main Pay), West Qurna 1 Field, Iraq. IR17, paper presented at the EAGE Work- shop on Iraq: Hydrocarbon Exploration and Field Development, Istanbul, Turkey
- Isaaks EH, Srivastava RM (1989) An introduction to applied geostatistics. Oxford University Press, New York
- Journel AG (1989) Geostatistical characterization of reservoir heterogeneities. In SEG annual meeting, Dallas, Texas, 29 October–2 November 1989
- Journel AG (1990) Geostatistics for reservoir characterization. SPE-20750-MS, presented at the SPE annual technical conference and exhibition, New Orleans, Louisiana
- Journel AG, Alabert FG (1990) New method for reservoir mapping. *J Pet Technol* 42(02):212–218
- Journel AG, Gomez-Hernandez JJ (1993) Stochastic imaging of the Wilmington clastic sequence. *SPE Form Eval* 8(01):33–40
- D. Kitching, Farmer R, Abuzaid M (2013) In search of the remaining oil in the “Main Pay” member of the Zubair Formation through surveillance oil mapping, Rumaila Field, Southern Iraq, Second EAGE Workshop on Iraq. doi:10.3997/2214-4609.20131456
- Liu Y, Harding A, Abriel W, Strebelle S (2004) Multiple-point simulation integrating wells, three-dimensional seismic data, and geology. *AAPG Bull* 88(7):905–921
- Massonnat GJ, Alabert FG, Giudicelli CB (1992) Anguille Marine, a deepsea-fan reservoir offshore Gabon: from geology to stochastic modelling. SPE-24709-MS paper presented at the SPE annual technical conference and exhibition, Washington, D.C., 4–7 October 1992
- Mikes D, Geel CR (2006) Standard facies models to incorporate all heterogeneity levels in a reservoir model. *Mar Pet Geol* 23:943–959
- Mohammed WJ, Al Jawad MS Al-Shamaa DA (2010) Reservoir flow simulation study for a sector in main pay-south rumaila oil field. SPE Oil and Gas India conference and exhibition, Mumbai, India
- Overeem I (2008) Geological modeling introduction: lecture, community surface dynamic modeling system. University of Colorado, Boulder
- Pyrzcz MJ, Deutsch CV (2014) Geostatistical reservoir modeling, 2nd edition. Oxford University Press, New York
- Seifert D, Jensen JL (1999) Using sequential indicator simulation as a tool in reservoir description: issues and uncertainties. *Math Geol* 31(5)
- Srivastava RM (1994) An overview of stochastic methods for reservoir characterization. In: Yarus JM, Chambers RL (eds) AAPG computer applications in geology no. 3, stochastic modeling and geostatistics: principles, methods and case studies, vol 316. American Association of Petroleum Geologists, Tulsa
- Walker RG (1992) Facies, facies models and modern stratigraphic concepts. Geological Association of Canada, St. John’s, pp 1–14
- Wells M, D Kitching, D Finucane, B Kostic (2013) An integrated description of the stratigraphy and depositional environment of the “Main Pay” member of the Zubair Formation, Rumaila, Iraq. IR21, paper presented at the Second EAGE Workshop on Iraq, Dead sea, Jordan. doi:10.3997/2214-4609.20131455
- White CD, Royer SA (2003) Experimental design as a framework for reservoir studies. SPE reservoir simulation symposium, Houston, Texas, USA
- Zhang T (2008) Incorporating geological conceptual models and interpretations into reservoir modeling using multiple-point geostatistics. *Earth Sci Front* 15(1):26–35